Research Article

Tao Meng*, Songsong Lian, Xiufen Yang, and Ruitan Meng

Effects of nano-modified polymer cement-based materials on the bending behavior of repaired concrete beams

https://doi.org/10.1515/ntrev-2021-0024 received March 27, 2021; accepted April 10, 2021

Abstract: As the use time of concrete structures increases, defects such as concrete cracks, corrosion and exposure of steel bars gradually appear, resulting in additional repair of concrete structures to increase their durability and life. In this article, the effects of nano-modified polymer cement-based materials as repair material on the bending behavior of repaired concrete beams were studied. Based on the moment, deflection, strain, surface quality and cracking development monitor of repaired concrete beams, the bending behavior of repaired beams with polymer, nano-modified polymer and fibers was compared and the failure mechanism of the beams was analyzed. The results showed that the nano-modified polymer cement-based materials are helpful in improving the performance of repaired beams, manifested by the increase in the ultimate bending moment and the significant improvement in the quality of the interface between repair and matrix concrete. Compared with polymer cementbased materials, nano-modified polymer cement-based materials result in a 27% increase in ultimate bending moment of the repaired beam and a 58% increase in cracking moment, while reducing the total number of cracks by 23% and the average width of cracks by 17% in the repaired beam. This article demonstrated the availability of nanomaterials for improving the loading behavior of structural components with polymer-modified cementbased materials.

Keywords: nano-modified polymer, repaired concrete beam, bending behavior

1 Introduction

Concrete is widely used as the main material in various construction projects including houses, bridges, tunnels and other structures. As the use time of concrete structures increases, defects such as concrete cracks, corrosion and exposure of steel bars gradually appear, which affect the safety of the structure. Thus, old buildings have started demanding additional repair and rehabilitation to increase their durability and life. For reinforced concrete beams, cracks appear in the tension area of concrete beams during the service process of the beam due to the low tensile strength of concrete. With time, these cracks lead to the corrosion of reinforcement, and the corrosion of steel bars can lead to concentration of internal stresses in the concrete and reduction in bond. resulting in further cracking and deterioration [1]. Therefore, it is necessary to study the new repair materials for the rehabilitation of reinforced concrete beams.

A good repair improves the function and performance of the structure, restores and increases its strength and stiffness, enhances the appearance of the concrete surface, provides water tightness, prevents ingress of the aggressive species to the concrete/steel interface and improves its durability [2]. Commonly used repair materials include cement, epoxy resins, polyester resins, polymer latex, etc. [3]. Polymer cement-based materials are widely used among the repair materials, which consist of a conventional cement mortar incorporating polymer latex [4].

Polymer cement-based materials attracted the attention of academia after a patent for adding natural rubber latex to road construction materials was obtained by

e-mail: taomeng@zju.edu.cn

Songsong Lian: College of Civil Engineering and Architecture, Zhejiang University, Hangzhou, China,

e-mail: 11712050@zju.edu.cn

Xiufen Yang: College of Civil Engineering and Architecture, Zhejiang University, Hangzhou, China, e-mail: 1660761671@qq.com Ruitan Meng: College of Civil Engineering and Architecture, Zhejiang University, Hangzhou, China; Architectural Design and Research Institute of Zhejiang University, Hangzhou, China, e-mail: mrt207@126.com

^{*} Corresponding author: Tao Meng, College of Civil Engineering and Architecture, Zhejiang University, Hangzhou, China,

Cresson in 1923 [5]. Polymer cement-based materials became popular as a construction material during the 1950s and was used to repair damaged concrete structures during the 1980s [6,7]. At present, polymer cement-based materials are being used in the repair and reinforcement of many projects such as hydraulic engineering, harbor engineering, highways, bridges and residential buildings. At the same time, some scholars have carried out related research on the application of polymers in repaired concrete. Pellegrino and Modena [8] used polymer-modified mortar to repair different areas of reinforced concrete beams and found that repairing the concrete compression area can improve the bending resistance of reinforced concrete beams; Assaad [9] applied polymers to repair projects and found that latex powder effectively improved the workability and bending behavior of cement-based materials. Mirza et al. [10] evaluated the performance of polymer-modified cement-based mortars for repairing surfaces of concrete structures up to a depth of 75 mm damaged due to exposure to cold climates. Polymer cement-based materials are widely used as repair material due to their good tensile resistance and strong adhesive force [11,12] and are beneficial in improving the interface of cement-based materials [13-15].

Moreover, many scholars have conducted related research on the modification of the polymer cement-based materials [16–20]. Fibers are often used to composite with polymer to improve the performance of cement-based materials. Xu et al. [19] demonstrated the compound effects of polyester fiber and SBR latex on the mechanical properties of concrete and found that polyester fiber reinforced the modification effects of the SBR latex, whereas the promotion of polyester fiber on the mechanical properties was also built up with the addition of the SBR latex. In addition to fibers, nanomaterials are also commonly used in the compounding and modification of materials, which show a series of excellent physical and chemical properties due to the small size effect, surface effect and macroscopic quantum tunneling effect [21]. Over the past few decades, researchers have made much progress by using nanomaterials to improve technical properties of cement-based materials [22-26]. The results showed that the mechanical properties and microstructure of the interface transition zone of cement-based materials were modified by nanomaterials due to their positive effect on the hydration process and pore structure [27–36]. Besides, Meng et al. [37] found that Nano-SiO₂ is helpful in improving the compressive strength and flexural strength of polymer cement-based materials in the early age due to the increase in hydration rate of cement.

It shows that nanomaterials are effective in modifying polymer cement-based materials.

Based on the above background, it is found that the polymer materials are a widely used repair material. Nanomaterials have great potential to modify polymer cement-based materials, and there are currently few studies about it. Thus, as a new potential repair material, the actual repair effect of nano-modified polymer cement-based materials on concrete structure needs further verification. Meanwhile, it is found that the polymer cement-based materials were used in the form of bonding directly in the existing research. In particular, there is no research to simulate the repair process of removing the old concrete and filling it with repair materials. Considering partial or total removal and replacement of concrete is unavoidable for severely damaged concrete, it is necessary to simulate the replacement of concrete with repair materials and investigate the performance of the concrete structure after repairing.

Therefore, the objective of this article is to verify the technical performance of nano-modified polymer cement-based materials as repair materials in the structural components and promote their wide application in the field of reinstatement construction. At the same time, this article simulates the real repair process after concrete damage in the tension zone of the beam and studies the technical performance of the repaired concrete beam, which has far-reaching reference value for actual engineering. Specifically, the effects of polymer, nano-modified polymer and fibers on the bending behavior of repaired concrete beams were compared and the failure mechanism of the beams was analyzed based on the moment, deflection, strain, surface quality and cracking development monitor of repaired concrete beams.

2 Experiment

2.1 Materials

P.O 42.5 cement produced by Anhui Conch Cement Company, sand of China's ISO standard produced by Xiamen Iso Sand Company, polycarboxylate superplasticizer with a water-reducing rate of 32% produced by Suzhou Xinlong Chemical Building Materials Company and defoamer (AGITANP803) produced by Germany MÜNZING Company were used. VK-S01B nano-SiO₂ dispersion was produced by Hangzhou Wanjing New Materials Company.

Table 1: Chemical composition of cement

| Composition | SiO ₂ | Al ₂ O ₃ | Fe ₃ O ₄ | CaO | MgO | SO ₃ | Na ₂ O |
|-------------|------------------|--------------------------------|--------------------------------|-------|------|------------------------|-------------------|
| wt% | 22.37 | 4.36 | 3.38 | 61.08 | 2.43 | 2.45 | 0.506 |

Polymer powder produced by Germany Wacker Chemie AG was made up of ethylene vinyl acetate (EVA) copolymer. The fiber material used in the test was polypropylene (pp) fiber produced by Shanghai Yingjia Industrial Development Company. The chemical composition of cement is shown in Tables 1–4 show the main properties of nano-SiO₂, polymer and fiber, respectively. The information in Tables 1–4 was provided by the manufacturers.

2.2 Experiment method

By testing the performance of reinforced concrete beams repaired by different materials, the effects of polymer, nano-modified polymer and fibers on the bending behavior of the beams were evaluated and compared. The test process is shown in Figure 1. The fluidity and mechanical properties of concrete were tested and the bending behavior of the beam was evaluated by the displacement at the supports and mid-span under various loads, tensile strain in the middle of the steel bar and compressive strain at the compressive edge of the concrete, ultrasonic

velocity of the repair layer, crack development, as well as the failure load and ultimate load of the beam.

2.2.1 Preparation of beams

The dimensions and reinforcement of the reinforced concrete beam are shown in Figure 2. The control concrete was poured first, which had a mix proportion of 360 kg cement, 1,116 kg gravel, 744 kg sand, 180 kg water and 3.6 kg polycarboxylate superplasticizer per cubic meter of concrete. After curing for 2 weeks, the repair materials made of self-compacting fine stone concrete with different proportions were casted into the lower part of the beams. The mix proportion of repair materials is shown in Table 5. The test beams were cured under the condition of temperature 20°C and humidity 55%.

2.2.2 Fluidity and compressive strength of concrete

The slump and T50 of concrete were measured according to "Technical Specification for Application of Self-compacting Concrete" (JGJ/T283-2012) [38]. By adjusting the amount of superplasticizer, the fluidity of the concrete was guaranteed to be basically the same, as shown in Figure 3. Samples with a size of 100 mm \times 100 mm \times 100 mm were prepared for the compressive strength test. According to "standard for test methods of mechanical properties on ordinary concrete" (GB/T50081-2019) [39], the compressive

Table 2: Physical and chemical properties of nano-SiO₂

| Outward | Solvent | Average diameter (nm) | SiO ₂ (%) | рН | Na ₂ O (%) |
|--------------------|---------|-----------------------|----------------------|------|-----------------------|
| Translucent liquid | Water | 13 | 30.1 | 10.2 | 0.32 |

Table 3: Technical indicators of polymer powder made up of ethylene vinyl acetate copolymer

| Solid content (%) | Apparent density (g/L) | Particle size (μm) | Minimum film forming temperature (°C) |
|-------------------|------------------------|--------------------|---------------------------------------|
| 99 | 540 | 0.5-8 | 4 |

Table 4: Technical indicators of pp fiber

| Density (g/cm ³) | Length (mm) | Diameter (µm) | Elongation at break (%) | Elastic modulus (GPa) | Tensile strength (MPa) |
|------------------------------|-------------|---------------|-------------------------|-----------------------|------------------------|
| 0.91 | 19 | 20 | 30 | 4.5 | 400 |



Figure 1: Test process.

strength of concrete samples was measured in triplicates at 14 days and 28 days of curing with a loading rate of 0.5 MPa/s.

2.2.3 Bending behavior of reinforced concrete beam

The bending behavior tests of the repaired beam were carried out when the repaired layer concrete was cured to the age of 14 days. The instruments and equipment used in the test included TS3860 strain gauge, force sensor, dial indicator, extensometer with 10 cm gauge length, jack, crack observer and ultrasonic detector, *etc*. The loading device and instrument layout of the test beam are shown in Figure 4.

According to "Code for Design of Concrete Structures" GB 50010-2010 [40], the ultimate load, normal service

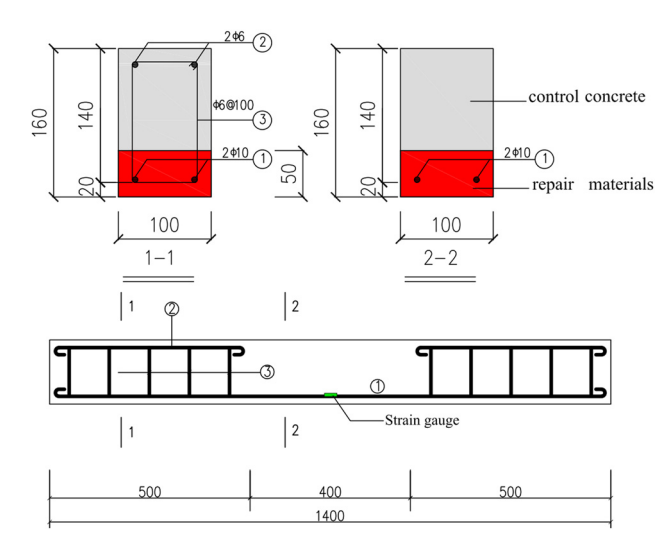


Figure 2: Dimensions and reinforcement of the reinforced concrete beam.

load and cracking load of the experimental beam were calculated. From equations (1) and (2), the ultimate bending moment can be calculated to be $4.84 \ \text{kN} \ \text{m}$. From equations (3) to (5), the cracking moment can be calculated to be $1.57 \ \text{kN} \ \text{m}$.

$$\alpha_1 f_{\rm ck} b x = f_{\rm vk} A_{\rm s}, \tag{1}$$

$$M_{\rm u} = \alpha_1 f_{\rm ck} bx \left(h_0 - \frac{x}{2} \right), \tag{2}$$

where $f_{\rm ck}$ and $f_{\rm yk}$, respectively, represent the axial compressive strength of concrete and the strength of steel bar; $A_{\rm s}$ represents the cross-sectional area of the steel bar in the tension zone; x represents the height of the concrete compression zone; b represents the width of the cross section; h_0 represents the effective height of the cross section; and $M_{\rm u}$ represents the ultimate bending moment.

$$I_0 = (0.083 + 0.19\alpha_{\rm E}\rho)bh^3, \tag{3}$$

$$y_0 = (0.5 + 0.425\alpha_{\rm E}\rho)h,$$
 (4)

$$M_{\rm cr} = \frac{\gamma_{\rm m} f_{\rm tk} I_0}{h - \gamma_0},\tag{5}$$

where I_0 represents the moment of inertia; $\alpha_{\rm E}$ represents the ratio of the elastic modulus of steel bar to that of concrete; ρ represents the longitudinal reinforcement ratio; $\gamma_{\rm m}$ represents the influencing coefficient of section resistance to plasticity; $f_{\rm tk}$ represents the axial tensile strength of concrete; and $M_{\rm cr}$ represents the cracking moment.

The experimental beams were loaded in stages with about 10% of the calculated ultimate load. When the load reached 90% of the calculated cracking load, the load was changed to 5% of the calculated ultimate load until the first crack appeared on the experimental beam. After exceeding the normal service load, the beam was

Table 5: Mix proportion of self-compacting fine stone concrete (kg/m³)

| Sample | Cement | Gravel | Sand | Water | Superplasticizer | Nano-SiO ₂ | EVA | Defoamer | Polypropylene fiber |
|--------|--------|--------|------|-------|------------------|-----------------------|------|----------|---------------------|
| В | 512 | 848 | 781 | 205 | 3.58 | _ | _ | _ | _ |
| Р | 512 | 848 | 781 | 205 | 1.24 | _ | 25.6 | 0.51 | _ |
| PS | 512 | 848 | 781 | 205 | 5.12 | 5.12 | 25.6 | 0.51 | _ |
| F | 512 | 848 | 781 | 205 | 3.58 | _ | _ | _ | 0.9 |

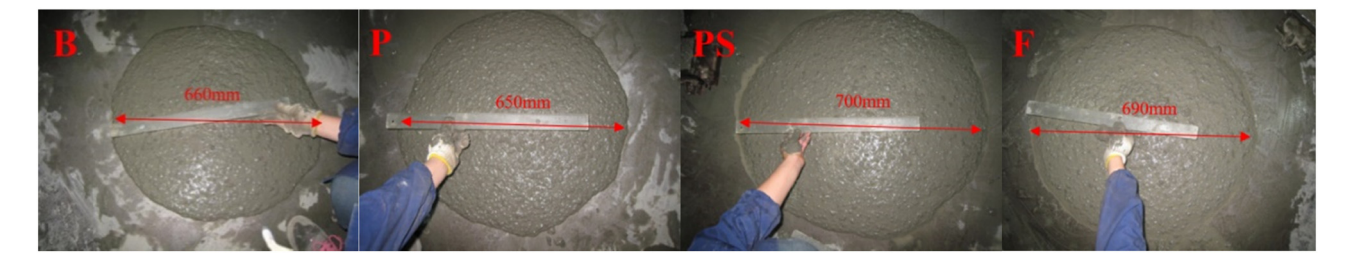


Figure 3: Spreading of fresh concrete.

continued to load at 10% of the calculated ultimate load. Finally, when it reached 90% of the ultimate load, the beam was continued to load until it reached the ultimate bearing state. According to this classification method, the load was divided into 11 levels. After the eleventh level of load, the beam was loaded to failure and the load at this time was the twelfth level. During the loading process, the measured data mainly include (1) the displacement of the support and the mid-span under various loads; (2) tensile strain at the middle of the main bar and compressive strain at the edge of the concrete under various loads; (3) ultrasonic velocity of repair layer under various loads; (4) the cracking moment of the beam and the development of cracks under various loads, including

crack distribution and maximum crack width; and (5) ultimate bending moment and ultimate compressive strain of concrete.

3 Results and discussion

3.1 Compressive strength

The compressive strength of the control concrete at the age of 14 days was 40.3 MPa. The compressive strengths of the repair materials at 14 and 28 days are shown in Figure 5.

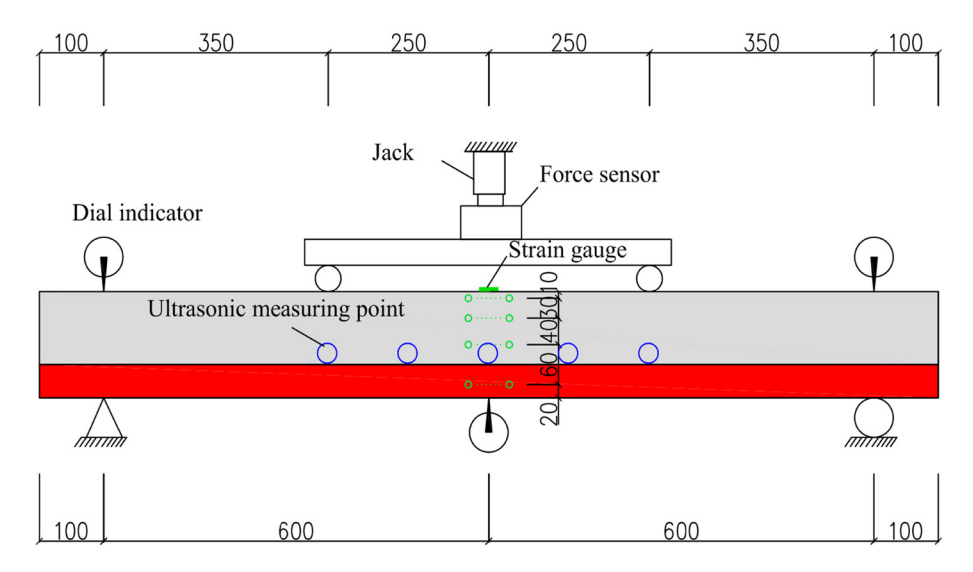


Figure 4: Illustrative diagram of beam bending behavior test of repaired beam.

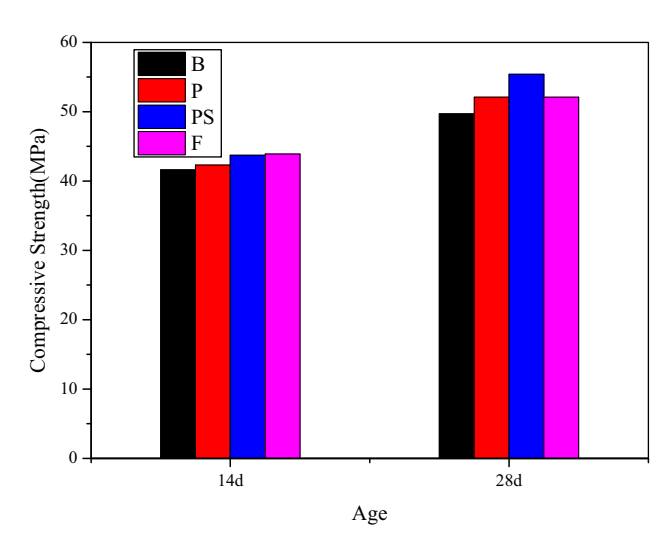


Figure 5: Compressive strength of repair materials.

When the concrete beam was loaded, the repair materials had been cured for 14 days and the control concretes had been cured for 28 days. The results showed that the compressive strength of the repair materials at the age of 14 days and that of the control concretes at the age of 28 days were approximately the same. Upon comparing the strength development of the repair materials, it could be found that the compressive strength of the four repair materials at the age of 14 days was relatively close. The compressive strength of the specimen PS at the age of 28 days was significantly higher than that of the other three specimens, indicating that the nanomaterials had an obvious effect in improving the compressive strength of concrete. Meanwhile, the compressive strength of specimens P and F was slightly higher than that of specimen B, indicating that the polymer and pp fiber played a beneficial role in the compressive strength of concrete.

3.2 Cracking load and ultimate bearing capacity

The repaired beams were loaded in stages and the cracking load and ultimate bearing capacity were measured, respectively, as shown in Table 6.

The bending moment when the first crack appeared was taken as the cracking moment. The theoretical calculation value of the cracking moment was 1.58 kN m. The cracking moments of B and P were smaller than the theoretical value. This was because the repair layer of the beam cannot be well integrated with the control layer and

Table 6: Cracking load and ultimate bearing capacity of reinforced concrete beams

| Sample | | mate bending ment (kN m) | Cracking moment (kN m) | | | |
|--------|-------|-----------------------------|------------------------|------------|--|--|
| | Value | Load level | Value | Load level | | |
| В | 6.77 | 12 | 0.94-1.38 | 3 | | |
| Р | 6.82 | 12 | 0.99-1.41 | 3 | | |
| PS | 8.66 | 12 | 1.57-1.85 | 4 | | |
| F | 6.93 | 12 | 2.17-2.37 | 5 | | |

the bonding surface changed the distribution and transmission of the force in the beam, resulting in the repair layer sharing more tension and cracking more easily. The cracking moment of PS was 58% larger than that of P. This was because nanomaterials not only had a good effect in improving material properties and interface bonding but also promoted the formation of polymer film in concrete, improving the bending and cracking resistance. The cracking moment of F was 38% larger than that of PS, indicating that the pp fiber had the most obvious effect in improving the cracking resistance of the repaired beam. This was because the fibers were distributed in random directions in the concrete, which dispersed the shrinkage stress and energy of the concrete to the fibers and weakened the plastic shrinkage stress effectively, thereby reducing the stress concentration at the crack tip and preventing the further expansion of the crack.

The theoretical calculation value of the ultimate bending moment was 4.84 N m. The ultimate bending moments of B, P, PS and F were 40, 41, 79 and 43% higher than the theoretical value. It can basically be determined that the actual strength of the tensile steel was higher than the design value, which made the experimental value higher than the theoretical value. Among them, the ultimate bending moment of the PS was the largest, which was 28% larger than that of B, 27% larger than that of P and 25% larger than that of F, indicating that the nanomaterials can modify the polymer cement-based materials and greatly improve the bending resistance of the repair beam.

3.3 Deflection

Figure 6 shows the relationship between the deflection of the repaired beam and the mid-span bending moment. It can be seen that when the load was small (before the

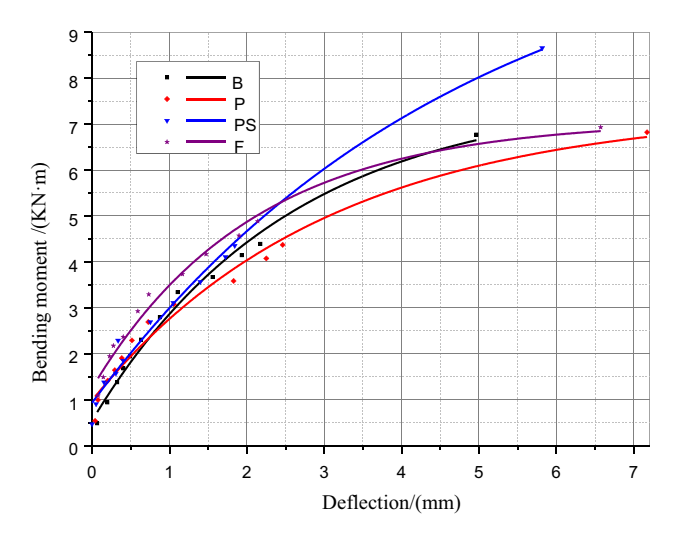


Figure 6: Relationship between the deflection and the bending moment of mid-span.

eighth load), the deflection of F was the smallest, while the deflection of other groups was not much different, indicating that the fiber materials were beneficial to controlling the deflection and deformation of the beam. When the mid-span bending moment was greater than 5 kN m, the deflection of PS was smaller than the other three groups, indicating that the nano-modified polymer cement-based materials can not only increase the strength of the repaired beam but also increase the rigidity. This was because the addition of nanomaterials has a beneficial effect on the formation of the polymer film and the properties of the bonding surface.

3.4 Strain development of concrete and steel

Figure 7 shows the tensile strain values of the main bars in the bending of different beams under various loads. Figure 8 shows the compressive strain values of different beams at the center of the upper concrete under various loads. It can be seen that the compressive strain of the concrete and the tensile strain of the steel bars had linear relationships with the bending moments, indicating that the compression zone of concrete and steel bars had not reached the yielding state from the beginning of loading to the beam failure. Therefore, the final failure of beams was not caused by the yield of steel bars or the failure of concrete, but mainly depended on the performance of the bonding surface. In other words, it was very important whether the force in the reinforced concrete beam can

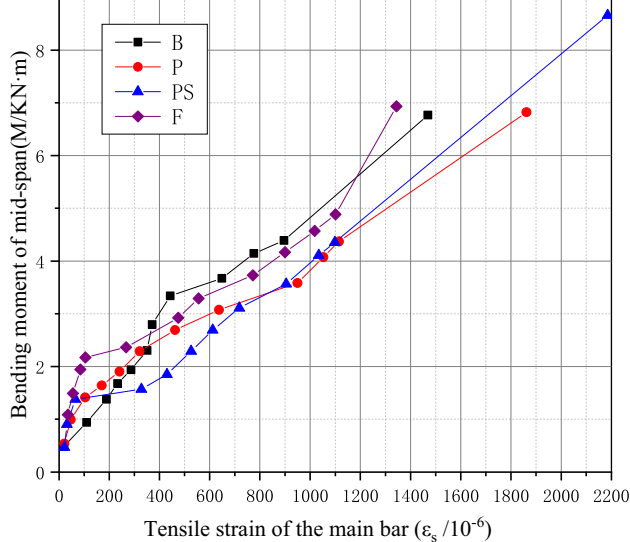


Figure 7: Tensile strain of the main bar in bending under various loads.

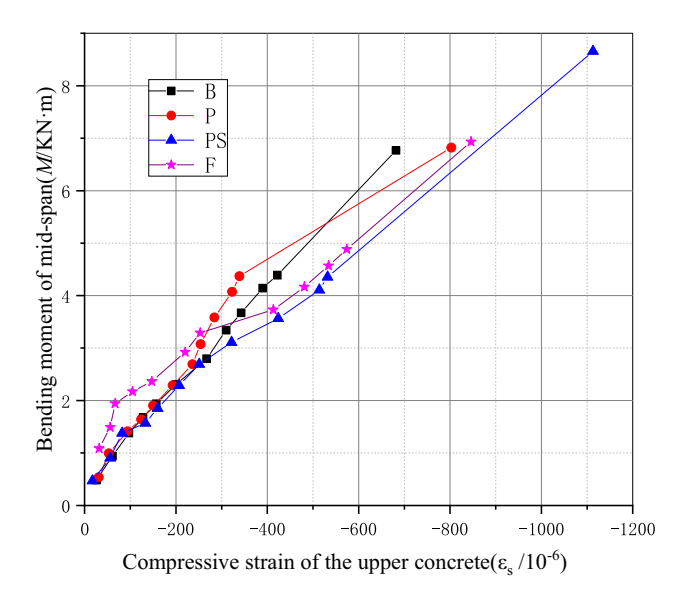


Figure 8: Compressive strain of the upper concrete under various loads.

effectively be distributed and transmitted on the bonding surface.

Figure 9 shows the strain at mid-span section of the concrete beam under different load levels before the beam fails. It can be seen that there was no linear relationship between the concrete strain of the beam and its corresponding height. This was because the bonding surface of the control layer and the repair layer of the reinforced concrete beam changed the force distribution and transmission, where the assumption that the section is

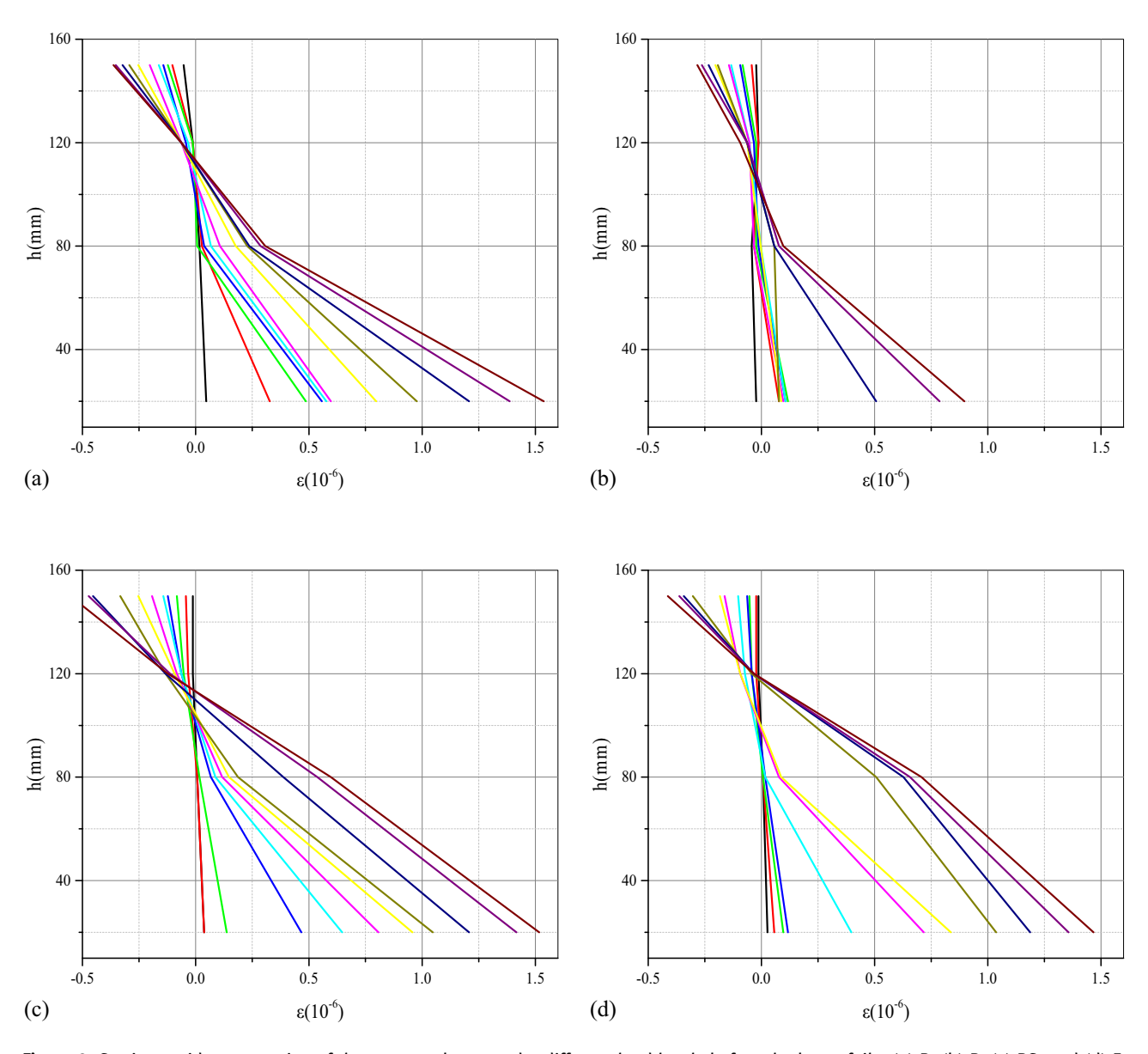


Figure 9: Strain at mid-span section of the concrete beam under different load levels before the beam fails. (a) B, (b) P, (c) PS, and (d) F.

plane was not satisfied. Among them, the relationship between the strain and its corresponding height of the concrete in group PS was the closest to linear, indicating that the use of nano-modified polymer cement-based materials can improve the integrity of the beam and the performance of the bonding surface.

3.5 Bonding quality of interfacial surface

The ultrasonic velocity of mid-span was used to characterize the bonding quality between the repair layer and the control layer. The ultrasonic velocity was recorded

after the load of each level was stabilized and five measuring points were tested, as shown in Figure 4. The results found that only the mid-span had a large change in ultrasonic velocity. Figure 10 shows the relationship between the ultrasonic velocity and the bending moment of mid-span. When the ultrasonic velocity was significantly reduced, it was determined that the bonding surface had slipped or separated.

As shown in the figure, the ultrasonic velocity of midspan of different beams fluctuated around 3,500–4,000 m/s before the bonding surface was separated. The ultrasonic velocities of B and F did not change significantly before the twelfth level loading. When the beams were loaded to failure, the ultrasonic velocities were found to reduce to

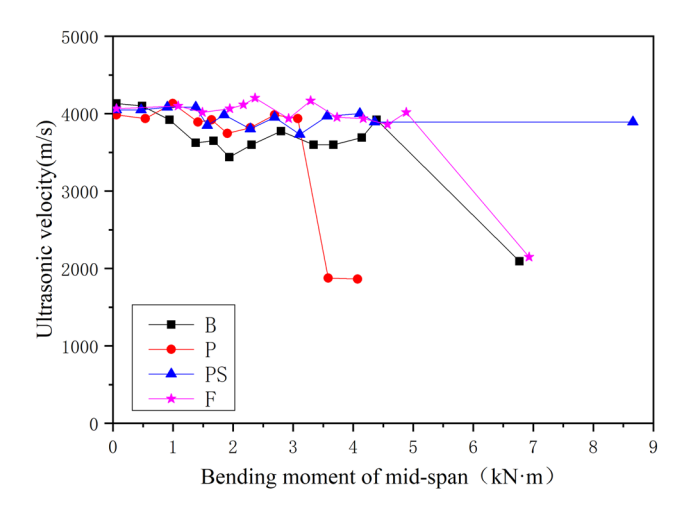


Figure 10: Relationship between bending moment of mid-span and ultrasonic velocity.

2,092 and 2,146 m/s, respectively, indicating that the bonding surface of B and F was separated at this time. When the beam of P was loaded to the ninth level, where the bending moment was 3.6 kN m, the ultrasonic velocity suddenly reduced to 1,876 m/s with the waveform reversed, indicating that the bonding surface had begun to separate before the beam was damaged. The ultrasonic velocity of PS was maintained between 4,166 and 3,846 m/s from the beginning of loading to failure, indicating that the bonding surface was always well bonded when the repaired beam was damaged. It can be seen that the nano-modified polymer cement-based materials can not only increase the ultimate bearing capacity of the repaired beams but also enhance the bonding surface, making the interface between the new and the old concrete well bonded.

According to the test results of bonding surface and deflection, the performance of bonding surface played an important role in the control of deflection. We found that the nano-modified polymer cement-based materials had a very good effect in improving the bonding force of the interface between the new and the old concrete, promoting the deformation well controlled under a large load.

3.6 Failure characteristics and crack morphology

Figure 11 shows the development of cracks in the repaired beam. There are generally two marks next to a crack. The first mark shows the position where the crack first appeared and the maximum width of the crack at this time and the number outside the parenthesis represents the loading level when the crack occurs. The second mark shows the position of the crack reached at the last loading level before the beam failure and the maximum width of the crack at this time. Table 7 summarizes the number, maximum width and average width of cracks in the concrete beams.

DE GRUYTER

For group B, the cracks developed mainly from the bottom of the concrete to the bonding surface, and the width of the cracks was relatively thick. The distribution of cracks presented the characteristics of more cracks in the lower part of the concrete and less in the upper part. For group P, the number of cracks was the largest and the distribution was the widest compared with the other groups. Moreover, in addition to cracks extending from the bottom of the concrete to the bonding surface, multiple cracks developed from the bonding surface to the upper part of the concrete. For group PS, there were cracks that developed upward from the bottom of the concrete and upward from the bonding surface. The total number of cracks in group PS was 23% less than that in group P, and the average crack width in group PS was 17% smaller than that in group P, indicating that the addition of nanomaterials can effectively control the development of cracks. At the same time, the upper and lower parts of the cracks in group B developed separately and rarely penetrated, which indicated that a certain amount of slip occurred at the bonding surface and the shear force could not be transmitted. The beam of group PS had cracks penetrating up and down, indicating that the interface has good bonding performance and can transmit shear force. This further proved that the nanomodified polymer cement-based materials can enhance the properties of the bonding surface.

3.7 Failure mechanism

According to the analysis of cracking moment, ultimate bending moment, deflection, tensile strain of steel bar, compressive strain of concrete, bonding surface and cracks, the failure process and failure mechanism of beams with different repair materials can be revealed.

The cracking and ultimate bending moments of F were higher than those of B, while the failure characteristics of B and F were similar. The steel bars and concrete of B and F did not yield. The bonding surface detached when the beams failed. The distribution of cracks presented the characteristics of more cracks in the lower part of the concrete and less in the upper part.

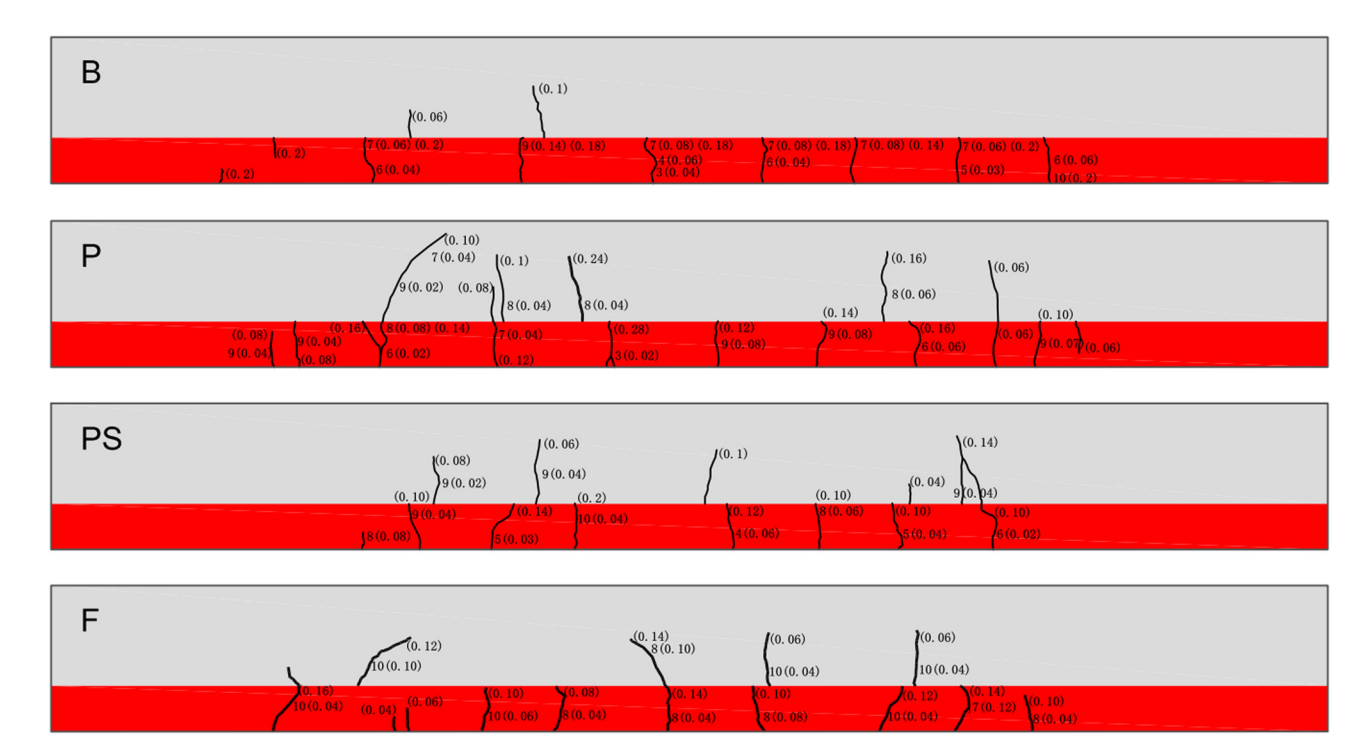


Figure 11: Development of cracks in the repaired beams.

Therefore, the failure mechanism of B and F was that the separation of the bonding surface of the repaired beam caused the unbalanced force distribution inside the beam.

The cracking load and ultimate bearing capacity of P had a certain increase compared with B. The steel bar and concrete had not reached yield. The bonding surface was partially separated under the ninth level of load and further expanded with the load. The number of cracks was the largest and the distribution was the widest. Taking into account that the tensile steel bars were located on the repair layer, the lower part of the control layer was subjected to the tensile force that should be borne by the steel bars after the bonding surface was partially separated, so that the cracks that developed upward from the bonding surface finally penetrated to

the top of the beam. Therefore, the failure mechanism of P was that the separation of the bonding surface of the repaired beam caused control layer to crack.

The beam of PS had the largest cracking load and ultimate bearing capacity. The steel bar and concrete had not reached yield, and the bonding surface had not separated. The respective developed cracks appeared on the upper and lower parts of the beam, indicating that the bonding surface may be misaligned.

4 Conclusion

The overall performance of the repaired reinforced concrete beam was related to the strength and toughness of

Table 7: Summary of cracks in concrete beams

| Sample | | Cracks in the l | ower part | | Cracks in the u | pper part | | acks | |
|--------|--------|------------------|------------------|--------|------------------|------------------|--------|------------------|------------------|
| | Number | Maximum width | Average width | Number | Maximum width | Average width | Number | Maximum width | Average width |
| В | 9 | 0.20 | 0.19 | 2 | 0.1 | 0.08 | 11 | 0.20 | 0.17 |
| Р | 11 | 0.28 | 0.12 | 6 | 0.24 | 0.12 | 17 | 0.28 | 0.12 |
| PS | 8 | 0.20 | 0.11 | 5 | 0.14 | 0.08 | 13 | 0.20 | 0.10 |
| F | 10 | 0.16 | 0.10 | 4 | 0.14 | 0.10 | 14 | 0.16 | 0.10 |

the repair material and the performance of the bonding surface. In this article, the effects of nano-modified polymer cement-based materials on the bending behavior of repaired concrete beams are mainly studied. Based on cracking moment, ultimate bending moment, deflection, tensile strain of steel bar, compressive strain of concrete, bonding surface and cracks, the bending behavior of concrete beams with different repair materials was compared and the failure mechanism of the beams was analyzed. The test results were as follows:

- (1) The addition of polymer can slightly increase the cracking moment and ultimate bending moment of the repaired beam, but cannot effectively improve the performance of the bonding surface, resulting in more cracks around the bonding surface.
- (2) The nano-modified polymer cement-based materials are helpful in improving the performance of repaired beams, manifested by the increase in the ultimate bending moment and the significant improvement in the quality of the interface between repair and matrix concrete. Compared with polymer cementbased materials, nano-modified polymer cement-based materials result in a 27% increase in ultimate bending moment of the repaired beam and a 58% increase in cracking moment, while reducing the total number of cracks by 23% and the average width of cracks by 17% in the repaired beam.
- (3) The addition of pp fiber can greatly increase the cracking load of the repaired beam and slightly increase the ultimate bearing capacity, as well as play a positive role in the deformation control of the repaired beam. Compared with nano-modified polymer cement-based materials, the cement-based material with pp fiber increased the cracking moment of the repaired beam by 38%, significantly improving the cracking resistance of the repaired beam.

In summary, the synergy of nano-SiO₂ and polymer can effectively improve the technical performance of the repaired concrete beam. Nano-modified polymer cementbased materials are helpful in improving the ultimate bending moment and cracking moment of the repaired beam and enhancing the performance of the bonding surface, thus reflecting a good repair effect. This article demonstrated the availability of nanomaterials for improving the loading behavior of structural components with polymermodified cement-based materials.

Funding information: The authors thank the support provided by the National Natural Science Foundation of China (52078453).

Author contributions: All authors have accepted responsibility for the entire content of this manuscript and approved its submission.

Conflict of interest: The authors state no conflict of

References

- Venkiteela G, Klein M, Najm H, Balaguru PN. Evaluation of the compatibility of repair materials for concrete structures. Int J Concr Struct Mater. 2017;11(3):435-45. doi: 10.1007/s40069-017-0208-5.
- Al-Zahrani MM, Maslehuddin M, Al-Dulaijan SU, Ibrahim M. Mechanical properties and durability characteristics of polymer-and cement-based repair materials. Cem Concr Comp. 2003;25(4-5):527-37. doi: 10.1016/S0958-9465(02) 00092-6.
- [3] Sánchez M, Faria P, Ferrara L, Horszczaruk E, Jonker HM, Kwiecień A, et al. External treatments for the preventive repair of existing constructions: a review. Constr Build Mater. 2018;193:435-52. doi: 10.1016/j.conbuildmat.2018.10.173.
- Huseien GF, Mirza J, Ismail M, Ghoshal SK, Hussein AA. Geopolymer mortars as sustainable repair material: a comprehensive review. Renew Sust Energ Rev. 2017;80:54-74. doi: 10.1016/j.rser.2017.05.076.
- Cresson L. Improved manufacture of rubber road-facing, rubber-flooring, rubber-tiling or other rubber-lining. Br Patent. 1923;191(474):12.
- [6] Akinyemi BA, Omoniyi TE. Engineering properties of acrylic emulsion polymer modified bamboo reinforced cement bonded composites. Eng Struct Tech. 2017;9(3):126-32. doi: 10.3846/2029882X.2017.1371085.
- Jamshidi M, Pakravan HR, Pourkhorshidi AR. Application of polymer admixtures to modify concrete properties: effects of polymer type and content. Asian J Civ Eng. 2014;15(5):779-87.
- [8] Pellegrino C, Modena C. Fiber reinforced polymer shear strengthening of reinforced concrete beams with transverse steel reinforcement. J Compos Constr. 2002;6(2):104-11. doi: 10.1061/(ASCE)1090-0268(2002)6:2(104).
- Assaad JJ. Development and use of polymer-modified cement for adhesive and repair applications. Constr Build Mater. 2018;163(FEB 28):139-48. doi: 10.1016/ j.conbuildmat.2017.12.103.
- [10] Mirza J, Mirza MS, Lapointe R. Laboratory and field performance of polymer-modified cement-based repair mortars in cold climates. Constr Build Mater. 2002;16(6):365-74. doi: 10.1016/S0950-0618(02)00027-2.
- [11] Fowler DW. Polymers in concrete: a vision for the 21st century. Cem Concr Comp. 1999;21(5-6):449-52. doi: 10.1016/S0958-9465(99)00032-3.
- [12] Kardon JB. Polymer-modified concrete: review. J Mater Civil Eng. 1997;9(2):85-92. doi: 10.1061/(ASCE)0899-1561(1997)9:2(85).
- [13] Jafari K, Tabatabaeian M, Joshaghani A, Ozbakkaloglu T. Optimizing the mixture design of polymer concrete: an

- experimental investigation. Constr Build Mater. 2018; 167(APR 10):185-96. doi: 10.1016/j.conbuildmat.2018.01.191.
- [14] Shehata N, Sayed ET, Abdelkareem MA. Recent progress in environmentally friendly geopolymers: a review. Sci Total Environ. 2020;762(5):143166. doi: 10.1016/ j.scitotenv.2020.143166.
- [15] Kim JH, Robertson RE, Naaman AE. Structure and properties of poly (vinyl alcohol)-modified mortar and concrete. Cem Concr Res. 1999;29(3):407–15. doi: 10.1016/S0008-8846(98) 00246-4.
- [16] Ozden S, Atalay HM, Akpinar E, Erdogan H. Shear strengthening of reinforced concrete t-beams with fully or partially bonded fiber reinforced polymer composites. Struct Concr. 2014:15(2):229–39. doi: 10.1002/suco.201300031.
- [17] Liu GW, Li SP, Gao F, Sun WZ, Xiao ZJ, Yang CF. An experimental study on static mechanical characteristics of the new modified polymer concrete with high strength and super lightweight using special polyurethane. International Conference on Sustainable Energy. Environment and Information Engineering (SEEIE); 2016 Mar 20–21. Bangkok, Thailand: DEStech Publications, Inc; 2016. p. 417–22.
- [18] El Maaddawy T, Soudki K. Carbon-fiber-reinforced polymer repair to extend service life of corroded reinforced concrete beams. J Compos Constr. 2005;9(2):187–94. doi: 10.1061/ (ASCE)1090-0268(2005)9:2(187).
- [19] Xu F, Zhou M, Chen J, Ruan S. Mechanical performance evaluation of polyester fiber and SBR latex compound-modified cement concrete road overlay material. Constr Build Mater. 2014;63:142–9. doi: 10.1016/j.conbuildmat.2014.04.054.
- [20] Sezen H. Repair and strengthening of reinforced concrete beam-column joints with fiber-reinforced polymer composites. J Comp Constr. 2012;16(5):499-506. doi: 10.1061/(ASCE) CC.1943-5614.0000290.
- [21] Zhang P, Wan JY, Wang KJ, Li QF. Influence of nano-SiO₂ on properties of fresh and hardened high performance concrete: a state-of-the-art review. Constr Build Mater. 2017;148:648-58. doi: 10.1016/j.conbuildmat.2017.05.059.
- [22] Liu CJ, He X, Deng XW, Wu YY, Zheng ZL, Liu J, et al. Application of nanomaterials in ultra-high performance concrete: a review. Nanotechnol Rev. 2020;9(1):1427–44. doi: 10.1515/ntrev-2020-0107.
- [23] Zhao ZF, Qi TQ, Zhou W, Hui D, Xiao C, Qi JY, et al. A review on the properties, reinforcing effects, and commercialization of nanomaterials for cement-based materials. Nanotechnol Rev. 2020;9(1):303–22. doi: 10.1515/ntrev-2020-0023.
- [24] Zhuang CL, Chen Y. The effect of nano-SiO $_2$ on concrete properties: a review. Nanotechnol Rev. 2019;8(1):562–72. doi: 10.1515/ntrev-2019-0050.
- [25] Du MR, Jing HW, Gao Y, Su HJ, Fang HY. Carbon nanomaterials enhanced cement-based composites: advances and challenges. Nanotechnol Rev. 2020;9(1):115-35. doi: 10.1515/ ntrev-2020-0011.

- [26] Ling YF, Zhang P, Wang J, Taylor P, Hu SW. Effects of nanoparticles on engineering performance of cementitious composites reinforced with PVA fibers. Nanotechnol Rev. 2020;9(1):504–14. doi: 10.1515/ntrev-2020-0038.
- [27] Ltifi M, Guefrech A, Mounanga P, Khelidj A. Experimental study of the effect of addition of nano-silica on the behaviour of cement mortars. Procedia Eng. 2011;10:900-5. doi: 10.1016/ j.proeng.2011.04.148.
- [28] Kafi MA, Sadeghi-Nik A, Bahari A, Sadeghi-Nik A, Mirshafiei E. Microstructural characterization and mechanical properties of cementitious mortar containing montmorillonite nanoparticles. J Mater Civil Eng. 2016;28(12):04016155. doi: 10.1061/ (ASCE)MT.1943-5533.0001671.
- [29] Hosseini P, Abolhasani M, Mirzaei F, Anbaran MRK, Khaksari Y, Famili H. Influence of two types of nanosilica hydrosols on short-term properties of sustainable white portland cement mortar. J Mater Civil Eng. 2018;30(2):04017289. doi: 10.1061/ (ASCE)MT.1943-5533.0002152.
- [30] Meng T, Ying KJ, Hong YP, Xu QL. Effect of different particle sizes of nano-SiO₂ on the properties and microstructure of cement paste. Nanotechnol Rev. 2020;9(1):833–42. doi: 10.1515/ntrev-2020-0066.
- [31] Meng T, Zhang JL, Wei HD, Shen JJ. Effect of nano-strengthening on the properties and microstructure of recycled concrete. Nanotechnol Rev. 2020;9(1):79–92. doi: 10.1515/ntrev-2020-0008.
- [32] Zhang P, Ling YF, Wang J, Shi Y. Bending resistance of PVA fiber reinforced cementitious composites containing nano-SiO₂. Nanotechnol Rev. 2019;8(1):690–8. doi: 10.1515/ntrev-2019-0060.
- [33] Chang TP, Shih JY, Yang KM, Hsiao TC. Material properties of portland cement paste with nano-montmorillonite. J Mater Sci. 2007;42(17):7478-87. doi: 10.1007/s10853-006-1462-0.
- [34] Sonebi M, Bassuoni MT, Kwasny J, Amanuddin AK. Effect of nanosilica on rheology, fresh properties, and strength of cement-based grouts. J Mater Civil Eng. 2015;27(4):04014145. doi: 10.1061/(ASCE)MT.1943-5533.0001080.
- [35] Nazari A, Riahi S. The effects of ZnO₂ nanoparticles on split tensile strength of self-compacting concrete. J Exp Nanosci. 2012;7(5):491-512. doi: 10.1080/17458080.2010.524669.
- [36] Meng T, Yu Y, Qian X, Zhan S, Qian K. Effect of nano-TiO₂ on the mechanical properties of cement mortar. Constr Build Mater. 2012;29:241–5. doi: 10.1016/j.conbuildmat.2011.10.047.
- [37] Meng T, Yu H, Lian S. Effect of nano-SiO₂ on properties and microstructure of polymer modified cementitious materials at different temperatures. Struct Concr. 2019;21(2):794–803. doi: 10.1002/suco.201900170.
- [38] China National Standards. Technical specification for application of self-compacting concrete. JGJ/T283-2012.
- [39] China National Standards. Standard for test method of mechanical properties on ordinary concrete. GB/T50081-2019.
- [40] China National Standards. Code for design of concrete structures. GB 50010-2010.